Hindawi
Wireless Communications and Mobile Computing
Volume 2022, Article ID 4319779, 15 pages
https://doi.org/10.1155/2022/4319779

Research Article

A Novel Design and Study of a Self-Complimentary Miniaturized Millimeter Wave Antenna for Body-Centric Networks

Turki M. Alanazi,[1] **Mohammad Monirujjaman Khan**,[2] **H. M. Arifur Rahman**,[2] **and Md Nakib Alam Shovon**[2]

[1]*Department of Electrical Engineering, College of Engineering, Jouf University, Sakaka, Saudi Arabia*
[2]*Department of Electrical and Computer Engineering, North South University, Bashundhara, Dhaka 1229, Bangladesh*

Correspondence should be addressed to Mohammad Monirujjaman Khan; monirkhan.qmul@gmail.com

Received 15 February 2022; Accepted 13 August 2022; Published 2 September 2022

Academic Editor: Farman Ullah

A new self-complimentary compact antenna operating at 60 GHz within the millimeter wave frequency range has been presented in this paper. The design is intended for the wireless body-centric network (WBCN). The proposed compact design has a dimension of $4.5 \times 6.03 \times 1.59\,mm^3$. The antenna was designed with multiple geometrical structures held upon a narrow feed line with a rectangular slot and parasitic elements to increase bandwidth. Free space simulations of the antenna produced optimistic results in terms of gain, radiation efficiency, and bandwidth; a maximum gain of 6.7 dB was achieved with an efficiency of 84.5%. Parametric studies were carried out to better understand its nature by modifying the key design aspects and comparing the outcomes. A 3D human torso phantom was virtually created with natural human body properties, and the on-body performance of the design was tested by placing the antenna in its near field. With some slight deviation from their peak performance, on-body simulations displayed better results in most of the cases. The antenna was positioned five different gaps from the torso for future investigations. The result of the distance-based study was amazingly good as the antenna performance was consistent throughout all distances. 10.77 GHz of bandwidth is found for the closest distance to the human torso, while the on-body radiation efficiency is also outstanding; the minimum radiation efficiency recorded is 73.78 when the antenna is just a couple of millimeters away. Overall, the comparison shows that the antenna worked best when it was placed only 2 mm apart from the body. Investigation indicates the antenna is a promising candidate for BCN applications because of its wider bandwidth and better on-body efficiency.

1. Introduction

For many good reasons, millimeter wave antennas grab numerous researchers' attention worldwide while looking for a suitable antenna for BCN or wireless body area networks (WBAN). Millimeter wave (mmWave) microstrip patch antennas have smaller physical dimensions; fit well in small electric devices and equipment; are lightweight, less power-consuming, and less complicated in structure, [1–3]; and are mostly suitable for short-ranged high speed and larger amounts of data transmission [4, 5]. Such properties make mmWave antennas potential candidates for body-centric networks. The mmWave frequency range extends from 30 GHz to 300 GHz, with wavelengths ranging from 10 mm to 1 mm [6–8]. Within this wide frequency range, several frequency bands are free for public use, which has made them more popular among others. Such a popular frequency is 60 GHz within the V-band spectrum, which was assigned as unlicensed by the FCC [9, 10]. But, there are certain challenges while using this frequency for communication, which is the high attenuation for atmospheric absorption. This limits its usage for long-distance communications [6, 10, 11]. However, for body-centric network applications, especially for advanced future healthcare facilities, 60 GHz can be implemented.

However, one big question mark still remains after the creation of a new millimeter wave antenna: will this antenna perform the same while it is in the near-field of a human

body? This becomes the more challenging part of designing a suitable antenna for WBAN or BCN. The performance of the antenna is influenced by the human body's capacitive nature, especially when the antenna is in its near-field. This effect can be noticed in almost all the antenna parameters, such as gain, efficiency, return loss, or bandwidth [12–14]. Sometimes, a perfectly tuned antenna behaves so bizarrely in the near-field of an organic body that it becomes ineligible to operate for human body near-field applications. The good news is that, in most circumstances, a few millimeters can prevent adverse effects on the human body.

Wireless communications find the human body to be an unwelcoming and frequently hostile environment. Human-to-human and human-to-self networking using wearable and embedded wireless sensors is referred to as body-centric wireless communications. WBAN, wireless sensor networks (WSNs), and wireless personal area networks (WPANs) are all included in this topic (WPANs). Advanced healthcare applications, smart home appliances, entertainment, security and identification systems, even in space exploration and military applications, all benefit from body-centric wireless communications [15]. Especially, in wearable computers, a field that focuses on high amounts of computer resources embedded with sensors and interfacing devices, connecting wears requires performing real-time and fast data transfer in the gigabytes per second range. These tasks could be simplified by implementing wireless body area networking (WBAN) with high-speed, contactless wireless data exchange.

In low-frequency operations, electromagnetic waves have greater penetration depth on human bodies [16–18]. But, for millimeter waves, the penetration depth is very low. The popular 60 GHz frequency of V-band has only a 0.5 millimeters of penetration depth on human body which cannot pass through the skin layer of the human body on most of the cases. But, it does not mean only half of a millimeter of the external part of the human body will affect an antenna's performance. Besides, the presence of the human body in close proximity to an antenna works as a catalyst and deviates the antenna's natural performance.

One of the most common fields of BCN or WBAN is the healthcare department, where a patient's vital physical signs are collected with wearable nodes with included antennas. These nodes, placed on different parts of the human body, keep them connected with each other and the master nodes connected with external data servers and online clouds. So, antennas in these systems must withstand their operability while in the near field of a human body. Other short-ranged communication may include connection between multiple devices within the indoor environments of hospital wards.

Few antennas for body-centric networks operating at frequencies lower than mmWave [19–25], i.e., ultra wideband, demonstrated promising results, but had larger physical dimensions. Among the recent research made on millimeter wave designs, few of them performed notably well. Chahat et al. presented and analyzed two printed antenna designs with the RT Duroid 5880 substrate with different techniques [26]; one of them is a linearly polarized antenna, and the other is a linearly polarized aperture coupled patch antenna. The antennas are made with a square-shaped substrate with a 10 mm × 10 mm dimension. Both the designs were tested on an artificially made torso phantom and performed well in terms of gain, efficiency, and SAR analysis.

A disc-shaped wearable antenna for body area networks was presented by Puskely et al. [27] and achieved a gain of 5.2 dB with at least 25% efficiency when positioned close to the human body. An antenna with a 14 mm × 10.5 mm physical size was presented by Wu et al., claimed to be more suitable for body-centric networks with higher gain [19] and a maximum of 63% on-body efficiency. A textile-mounted PIFA antenna was presented by Vilas S. Ubale and Lamba, which was innovative and comfortable for BAN applications and had an operating frequency of 2.45 GHz [28]. Jiang et al. proposed a circularly polarized flexible design for wireless body area network (WBAN) which they claimed to be highly efficient with a maximum efficiency of 79% and 5.2 dB of gain [29]. Brizzi et al. presented two antennas with electromagnetic band gaps with two different structures: cylindrical structures and woodpile planar designs for body area networks operating at 60 GHz frequency [30]. The antennas showed directivity of 7.55 dBi and 6.72 dBi, respectively. According to the authors, the first antenna is better suited for on-body applications. Alibakhshikenari et al. have presented several millimeter wave antenna and array designs [2, 31–36] with unique design methods and techniques. In one research authors proposed a beam scanning leaky wave antenna (LWA) which operates on 55 GHz to 65 GHz. The antenna was designed by the authors using metamaterials and a composite right/left handed transmission line (CRLH-TL).

Except for those mentioned above, a little other research on millimeter wave body area network antennas like [6, 37–39] also produced promising results. This paper proposes a millimeter wave patch antenna design intended for the body-centric network (BCN). Antenna design, free space simulation, parametric study, on-body simulation, distance-based study, and conclusion are the other aspects of the work. The work is divided into seven pieces altogether. The first section discusses on millimeter wave, BCN, and BAN with a few related recent works. The antenna construction is presented and explained in Section 2. Sections 3 and 4 present, respectively, the results of the parametric investigation and the free space simulation. On-body simulation results are evaluated at a distance in Sections 5 and 6. The simulations are used to establish a conclusion in the last portion.

2. Antenna Design

The popular electromagnetic element design and simulation program computer simulation technology (CST) Microwave Studio Suite, which runs on Microsoft Windows, was used to build and simulate the proposed antenna. The antenna is made with a self-complementary design. The radiator patch of the antenna consists of two "U"-shaped bricks placed face-to-face with a chain-like arrangement within a square slot inside a circle. This shape on the top of the antenna has been chosen due to the impedance matching and wider impedance bandwidth of the antenna. There is a slot on

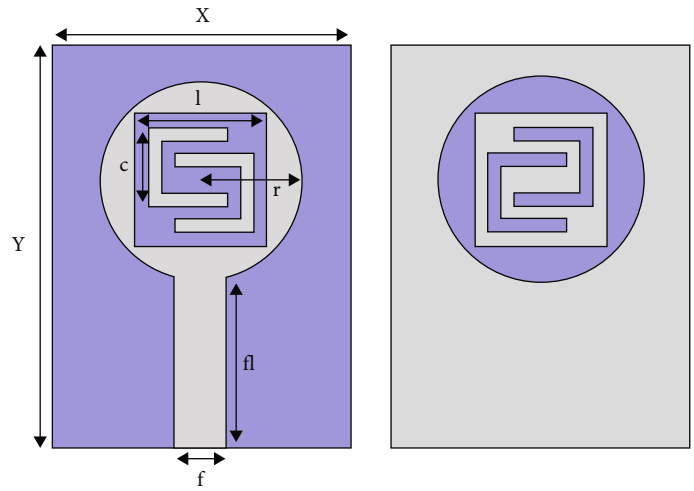

Figure 1: Antenna dimensions.

the ground plane of the antenna, and this was done to obtain the impedance matching and wider bandwidth. Having a ground plane on the backside of the antenna will provide a shield between the antenna and the human body, which will have less effect on the antenna parameters from the human lossy body tissues.

The antenna with the substrate is 9.42 mm long and 4 mm wide. The electrical size of the antenna over the length and width of the substrate of the antenna is 0.53λ and 1.25λ, respectively. The circular patch of the radiator has a radius of 1.5 mm. The square slot has a side length of 4.5 mm on each side. The U bricks have a width of 0.28 mm. The main circular shape is connected to the waveguide port with a feed line. The length of the feed line is 2.57 mm, which is denoted as "fl" in Figure 1, and the width of the feed is $f = 0.8$ mm. The impedance matching of the antenna can be varied by changing the width of the feedline of the antenna. The frequency shifting is possible by changing the size of the circular shape of the radiating element of the proposed antenna.

Table 1 shows the dimensions of the different parts of the antenna, where "x" and "y" are the length and width of the antenna, respectively. Values for the other parameters of Figure 1 can also be found in the table.

Similarly, in Table 2, the thickness of the different layers of the antenna, their materials, and their corresponding permittivity are shown. The material used for the ground and the patch radiator is PEC (perfect electric conductor). Both the layers have a similar thickness of 0.035 mm. The antenna substrate is made of Rogers RT6002 with a dielectric constant of 2.94. Rogers RT6002 has an excellent dimensional stability, and, due to its low-loss property, it is suitable for getting resonant point at higher frequency ranges. Because of this, RT6002 was selected as the substrate material [40–42]. 1.52 mm thick is the substrate layer. Since the ground and the radiator patches are made of perfect electric conductors, their relative permittivity could not be defined.

Figure 2 depicts views of the antenna taken from various angles. Figures 2(a) and 2(b) show the antenna as seen from the front and back, respectively. The antenna's right view and left view are shown in Figures 2(c) and 2(d), respectively. Figures 2(e) and 2(f) depict the antenna from the front and back in three dimensions, with the various layers denoted.

Table 1: Dimensions of the antenna.

S. no.	Parameter	Value (mm)
1	x	4.50
2	y	6.03
3	l	2.00
4	c	1.20
5	r	1.50
6	f	0.80
7	fl	2.57

Table 2: Materials for antenna.

Parameter	Thickness (mm)	Material	Epsilon
Ground	0.035	PEC	—
Substrate	1.52	Rogers RT6002 (loss free)	2.94
Patch radiator	0.035	PEC	—

3. Free Space Simulations

A waveguide fed port was used to excite the antenna for simulations. The port is attached to the bottom surface of the antenna structure, touching the feedline of the radiator and the substrate. The dimension of the port is 3.84×2.305 mm^2. Before starting simulation, open space boundary has been selected with $\lambda/4$ mm of added space from the structure on each surface. For far field simulation, 10 mm of space was accounted for on each surface.

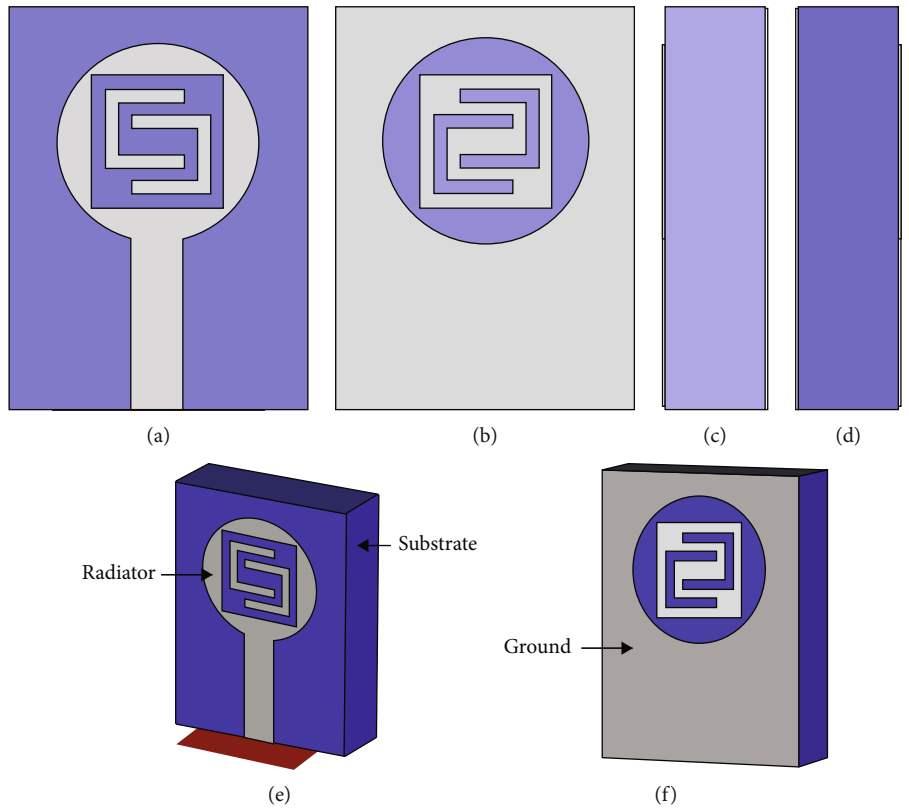

Figure 2: Antenna design: (a) frontage view, (b) rear view, (c) right view, (d) left view, (e) perspective frontage view, and (f) perspective rear view.

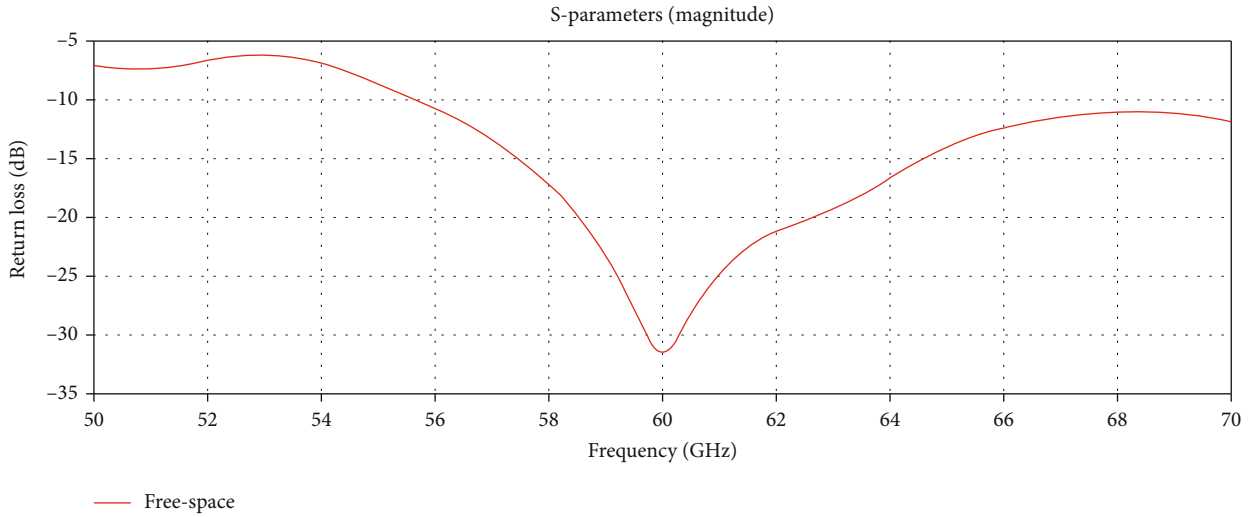

Figure 3: Return loss for free-space.

3.1. Return Loss. Within the frequency range of 50 GHz to 70 GHz, the antenna was modelled in free space. The frequency response is provided below. Figure 3 displays the antenna's return loss performance across the simulated frequency range. At 60 GHz, the resonance can be observed. The antenna becomes operational with less than -10 dB return loss from 57.5 GHz and remains under -10 dB line up to the upper simulated frequency limit. The return loss was found to be -31.45 dB at 60 GHz.

3.2. 3D Radiation Patterns. Figure 4 shows the 3D radiation pattern of the antenna with the transparent pattern and visible antenna structure on the left image and without the structure on the right. The antenna shows maximum gain along the direction of the Y axis with a value of 6.71 dB.

3.3. 2D Radiation Patterns. Two-dimensional radiation patterns on the XY plane and the YZ plane, correspondingly, are shown in Figures 5(a) and 5(b) at 60 GHz. The principal

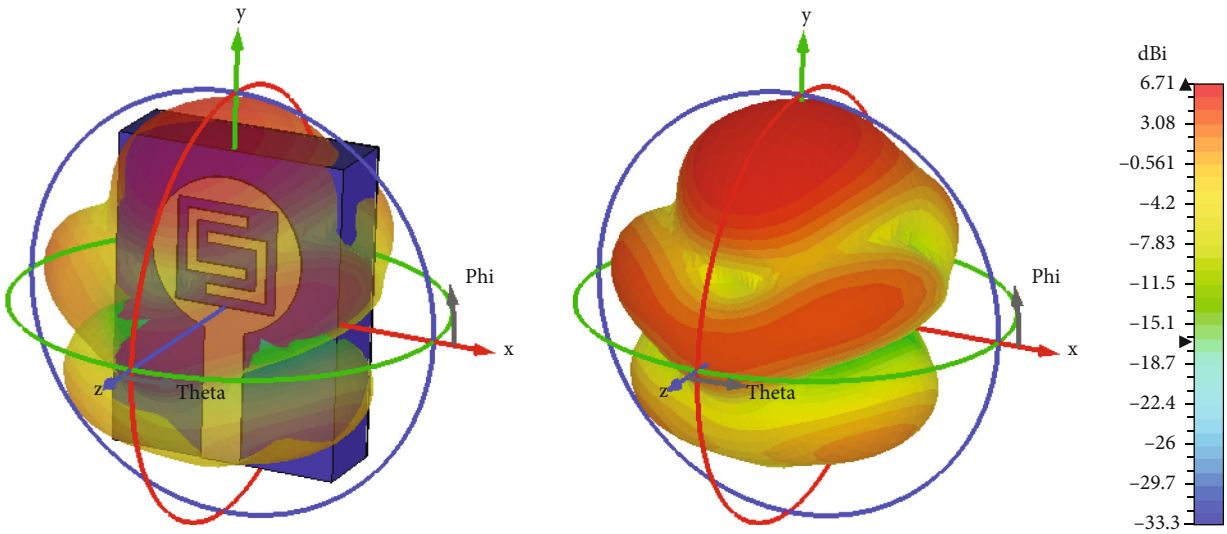

Figure 4: 60 GHz free space 3D radiation pattern.

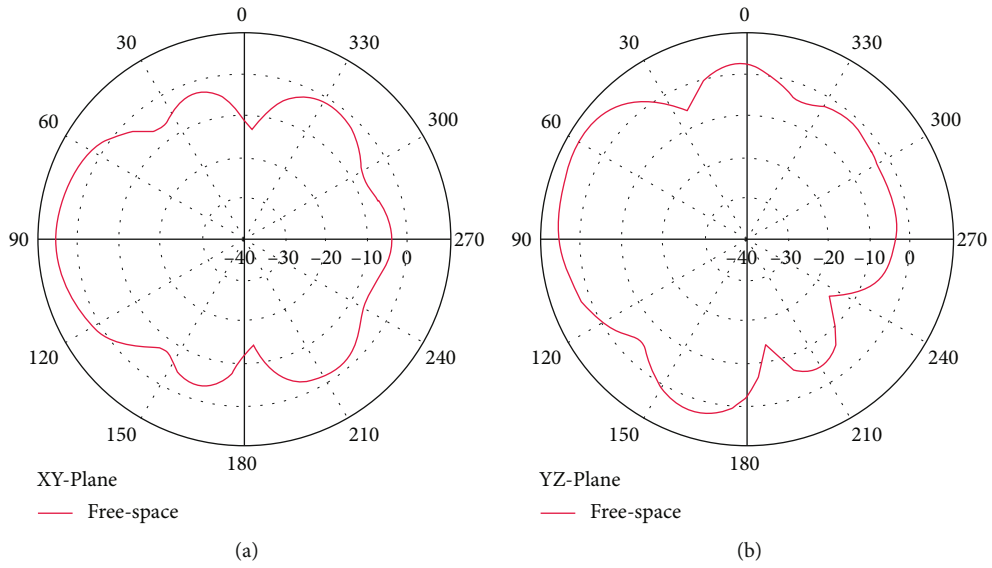

Figure 5: The XY plane and the YZ plane in free space: a 2D radiation pattern for 60 GHz.

lobe orientation of the antenna's radiation pattern in the XY plane is 90 degrees. In the YZ plane pattern, the major lobe orientation is about 60 degrees.

3.4. Analysis of the Surface Current. When the antenna is engaged at a 60 GHz frequency using "port 1," Figure 6 shows the surface current distribution. In the area between the ground plane and the radiator patch, the peak density was 148 amps per meter. At the resonant frequency, Quasi TEM mode propagation was detected at the waveguide excitation.

3.5. VSWR. The antenna's voltage standing wave ratio (VSWR) is shown in Figure 7. At the resonant frequency, the VSWR value is less than 1.1, which is very near to the optimum value.

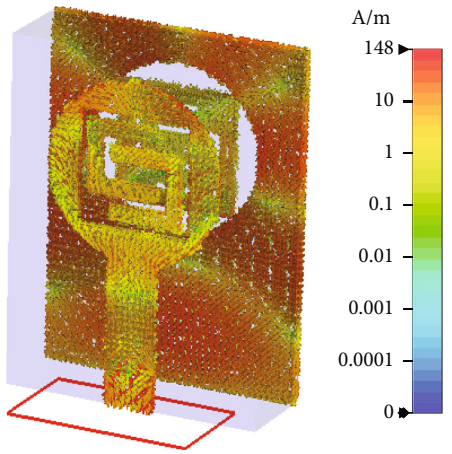

Figure 6: For 60 GHz, the available surface current.

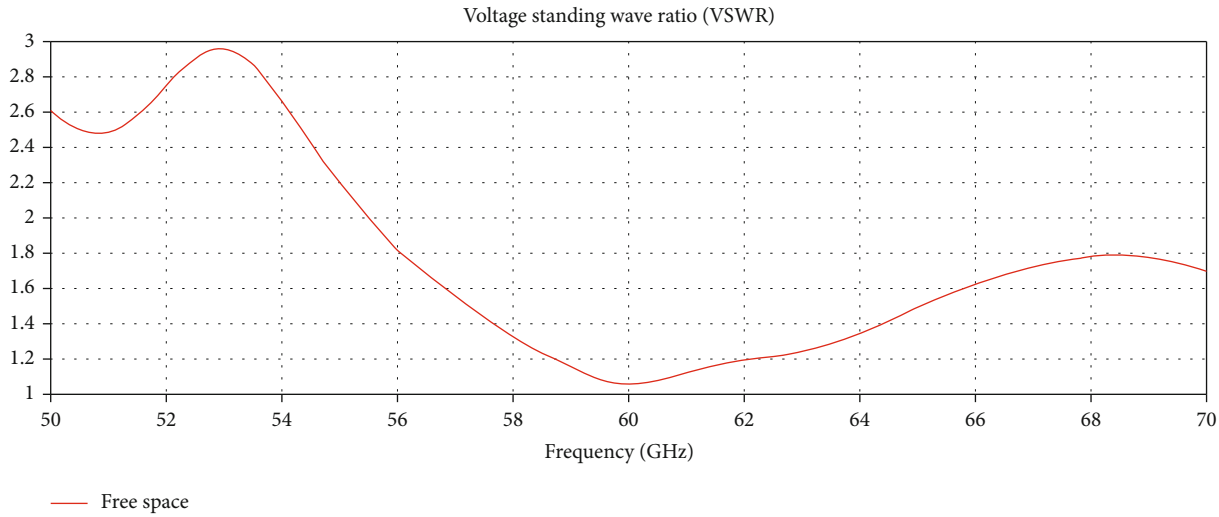

Figure 7: VSWR for free space 60 GHz.

3.6. Efficiency vs. Frequency. Figure 8 shows how the radiation efficiency changes with respect to frequency. Although higher efficiencies can be noticed in other frequencies around 60 GHz, yet it shows more than 84 percent of efficiency in our desired frequency.

3.7. Gain vs. Frequency. Figure 9 presents the maximum gain vs. frequency curve. The gain has gradually increased from 52.5 GHz to 57 GHz but has slightly decreased around 61 GHz before reaching its maximum. Although slightly higher gains can be seen in other frequencies, it still produces 6.7 dBi of gain at our selected frequency of 60 GHz.

4. Parametric Study

The parametric research was conducted after the free space simulations with the previously mentioned dimensions in order to understand the nature of the design and how it affects the output results. The measurements were changed, the simulation was run again, and the results were compared to the base results. The parametric study was done based on the changes in their corresponding return loss response curves. To achieve this, the antenna dimension was altered by varying the antenna substrate's width, which also altered the antenna's overall size.

In Figure 10, return losses are plotted for changing the width of the substrate by first decreasing and then increasing by 0.5 mm. When the substrate's length was reduced to 4 mm, the resonance frequency was slightly displaced to the right, and the green curve shows the antenna's return loss at that point. Similarly, increasing it to 5 mm (blue curve) tilts it to the right. In both cases, return loss values increased more than the original curve found for the original design. When the design is reverted back to the original design, the length of the substrate is varied in a similar manner. The length of the substrate "y" is first decreased to 6 mm and then increased to 6.05 mm.

In the above, Figure 11 presents the return loss responses when the antenna substrate length is changed. The green curve represents the return loss when the length is reduced by 0.03 mm. In this case, the return loss curve is slightly right-shifted with respect to the resonant point. The RL value at 60 GHz remains almost identical to the original design's plot. When the length is increased by 0.02 mm (blue curve), the resonant point is slightly left-shifted. The RL value is also reduced for this scenario.

The antenna's feed width, "fw," is changed after the preceding alteration is made in order to see how it affects the return loss curve. The original feed width was 0.8 mm wide. It was first reduced to 0.6 and the simulation result was plotted. The green line in the above figure (Figure 12) represents the return loss curve for the reduced feed width design, which degrades the RL value and shifts the curve to the right. Then, the feed width is made wider and kept at 1 mm. The blue curve in the figure shows the return loss for this scenario, where the resonant point is slightly left-shifted. The RL value at the selected frequency is somewhat similar to the original design.

A few other tests on the antenna were performed to justify its basic design, such as when the "U"-shaped parasitic elements were not present or when there was no slot at all on the radiator patch. This test also includes the justification of the ground plane's role. The following table presents the test results.

Table 3 shows the antenna parameters when the radiator patch is missing the "U"-shaped parasitic elements and the ground plane. It also shows the change in antenna behavior if the patch remains unslotted. All the parameters are compared with the free space. In all the scenarios, the resonant point deviates from the desired 60 GHz. However, the original design produces more optimized gain and efficiency while keeping the resonant point at 60 GHz.

4.1. Comparison. The table given below summarizes the results of all the parametric studies done above. The results were compared in terms of gains, efficiencies, bandwidths, and return losses. The above parametric study produces

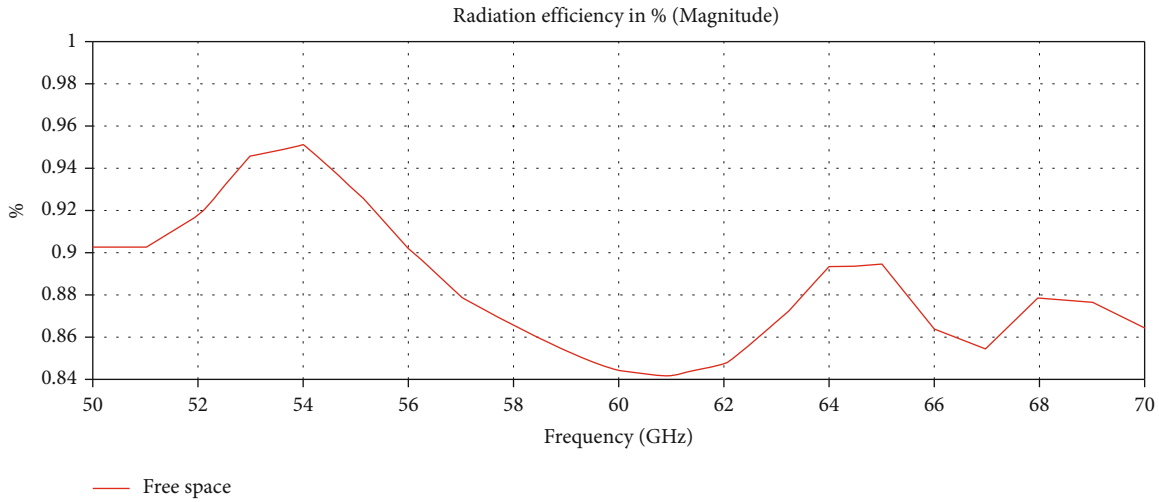

Figure 8: Efficiency vs. frequency.

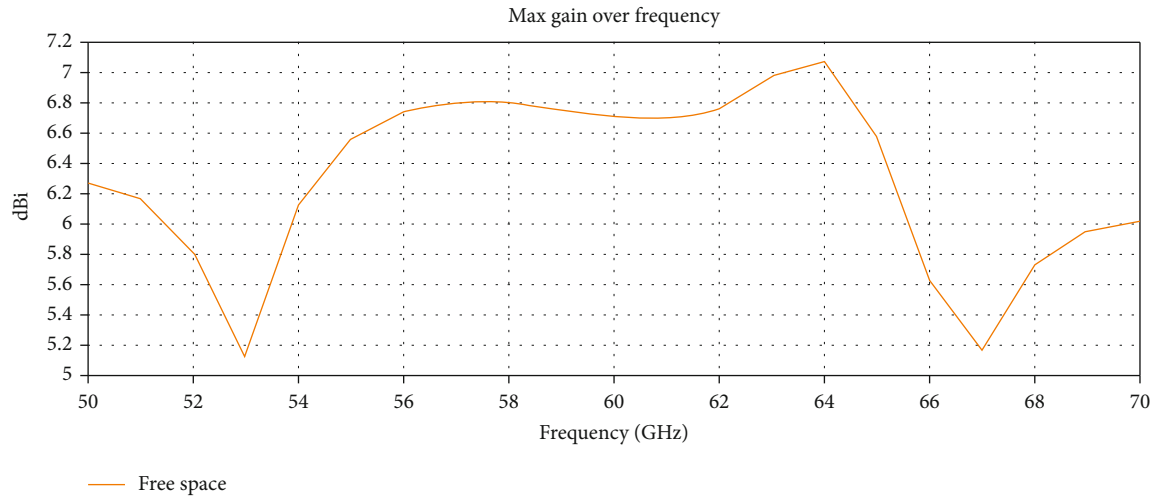

Figure 9: Maximum gain vs. frequency.

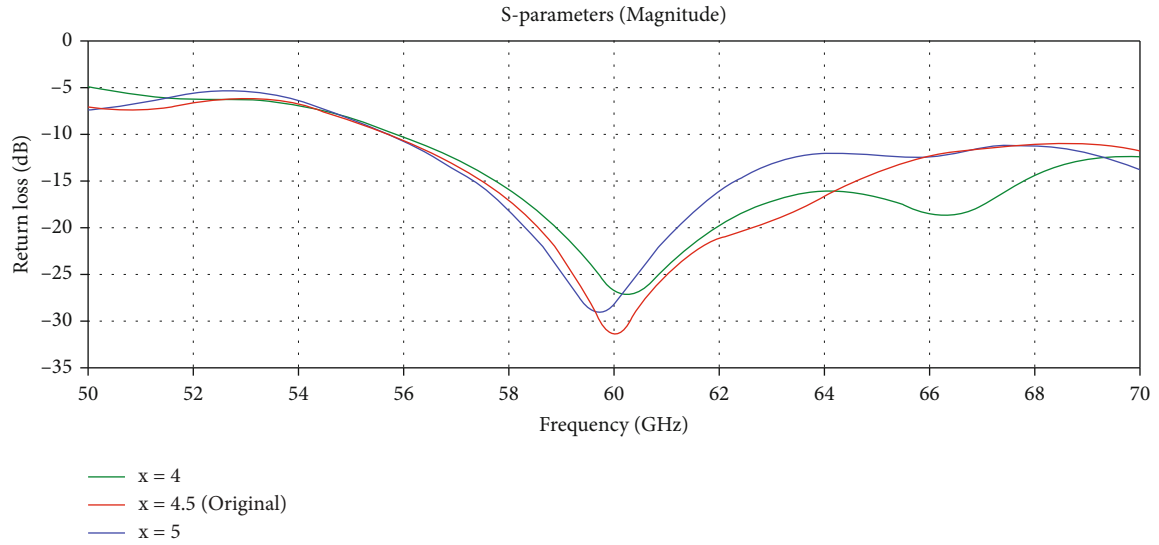

Figure 10: Comparison of return loss for various x values.

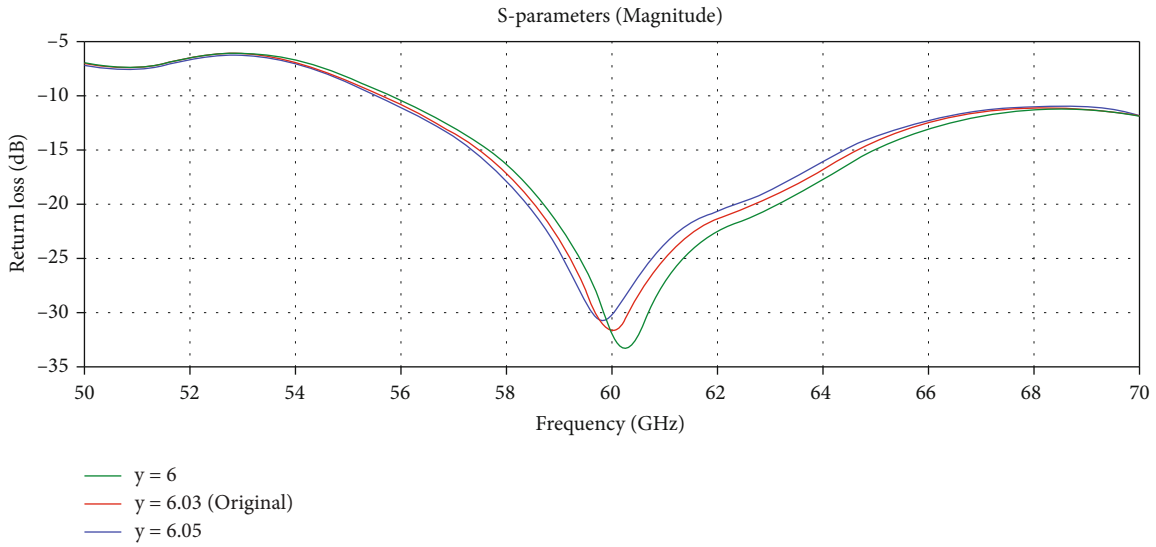

Figure 11: Return loss comparison with different y values.

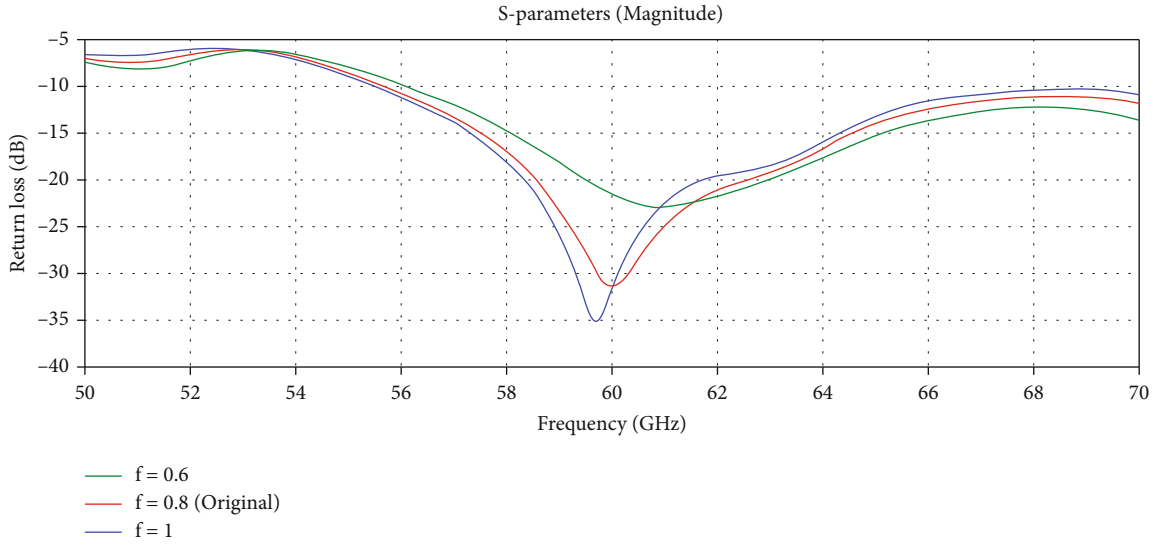

Figure 12: Return loss comparison with different "f" values.

Table 3: Justification of the basic model.

Parameter	Original design	Without parasitic elements	Without slot (solid patch)	Without ground plane
Center frequency (GHz)	60	61.52	59	70
Bandwidth (GHz)	—	—	—	—
Gain (dBi)	6.712	5.081	7.958	6.566
Radiation efficiency (%)	84.48	86.10	87.85	92.02

the results shown in Table 4. The results are compared with the free space simulation findings. In the case of changing the substrate dimensions, it could not produce better results than the original design. In one case, the feed width modification made the return loss lower than the original but shifted the resonant frequency from the desired point. Therefore, the original design produces more appropriate and acceptable results for the 60 GHz frequency.

Table 4: Analytical study.

Parameters	Free-space	$x = 4$	$x = 5$	$y = 6$	$y = 6.05$	$f = 0.6$	$f = 1$
Return loss (dB)	-31.45	-26.63	-28.18	-31.47	-30.10	-21.56	-31.77
Bandwidth (GHz)	—	—	—	—	—	—	—
Gain (dBi)	6.712	6.675	7.006	6.744	6.690	6.806	6.644
Radiation efficiency (%)	84.48	87.57	84.97	84.64	84.50	84.24	85.09

Table 5: Torso phantom dimension values.

Parameter	Length (mm)	Width (mm)	Thickness (mm)	Relative permittivity	Conductivity (S/m)
Skin	12	10	2	7.9753	36.397
Fat	12	10	3	3.1324	2.8152
Muscle	12	10	4	12.856	52.825

5. On-Body Performance Test

The antenna was tested on a computer-generated, three-dimensional human torso phantom because it is meant to be used in a WBAN. The muscles, fat, and skin that make up the human body's top three layers made up the phantom. Three layers are layered on top of each other; the muscle layer is the thickest, measuring 4 millimeters in thickness. The fat layer, with a thickness of 3 millimeters, is next put between the muscle and the skin. The skin is the outermost layer, positioned above the muscle. This is the thinnest layer among the others. The average layer thickness of the human body was used to choose these thicknesses at random. They are created by taking use of the layers' electromagnetic properties. These three layers together form the torso phantom, which measures 12 mm in length and 10 mm in width. The torso is depicted graphically in Figure 10. Then, the torso phantom was mounted with the novel antenna design that was previously shown, and its performance was evaluated by duplicating all of the findings. The results were next contrasted with those found in a free-space simulation. The dimensions and electromagnetic properties of the torso phantom's three levels are presented in the table below. In Table 5, the dimensions of the different layers are given one by one. The relative permittivity of the materials used for skin, fat, and the muscle layers is 7.96, 3.13, and 12.86, respectively. The conductivity of the material is also given in siemens per meter.

Figure 13 depicts the side view of the virtually created human torso model where the three different layers of skin, fat, and muscle are shown.

5.1. Overbody Return Loss. The antenna's on-body return loss is depicted in Figure 14 in the figure above. A 4-millimeter distance to the body was taken into account to replicate this. The bandwidth and return loss have both decreased as a result of the human body effect, although the RL value is still significantly below -10 dB. The on-body bandwidth was found to be around 10 dB for a distance of 4 mm.

5.2. On-Body VSWR. The antenna's on-body voltage standing wave ratio is shown in Figure 15, while the antenna is kept 4 mm away from the torso. The VSWR value at the desired 60 GHz frequency was found to be below 1.7 for the on-body simulation, which stays in the acceptable region as long as it is below 2.

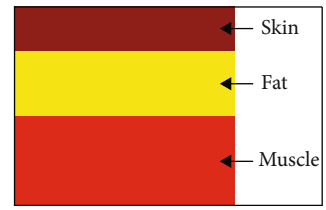

Figure 13: Torso phantom.

5.3. Pattern of On-Body Radiation. The original model for the antenna's on-body performance used 4 mm as the standard distance from the human torso. Figure 16 shows a simulated 3D far-field radiation pattern with and without the structure when the proposed antenna is placed 4 mm from the torso phantom. The maximum increase on the x-axis was measured at 6.67 dBi.

5.4. On-Body 2D Radiation Patterns. In Figure 17, 2D radiation patterns of the antenna are presented when the antenna is placed 4 mm close to the human torso phantom. Figure 17(a) is the pattern on the XY plane, where the on-body radiation pattern looks very much similar to the free space pattern. There is almost no change in lobe directions and gains. In Figure 17(b), the on-body pattern was slightly deviated from the free space result which is expected.

6. Distance-Based Study

To further understand the antenna's performance on the human body, it was put over the torso at five different distances and simulated to see how its performance changed. The torso phantom is separated by 2 mm, 4 mm, 6 mm, 8 mm, and 10 mm.

Figure 18 shows the antenna's placement above the chest at different heights. Antenna parameters were investigated for each distance using different simulations, and they were

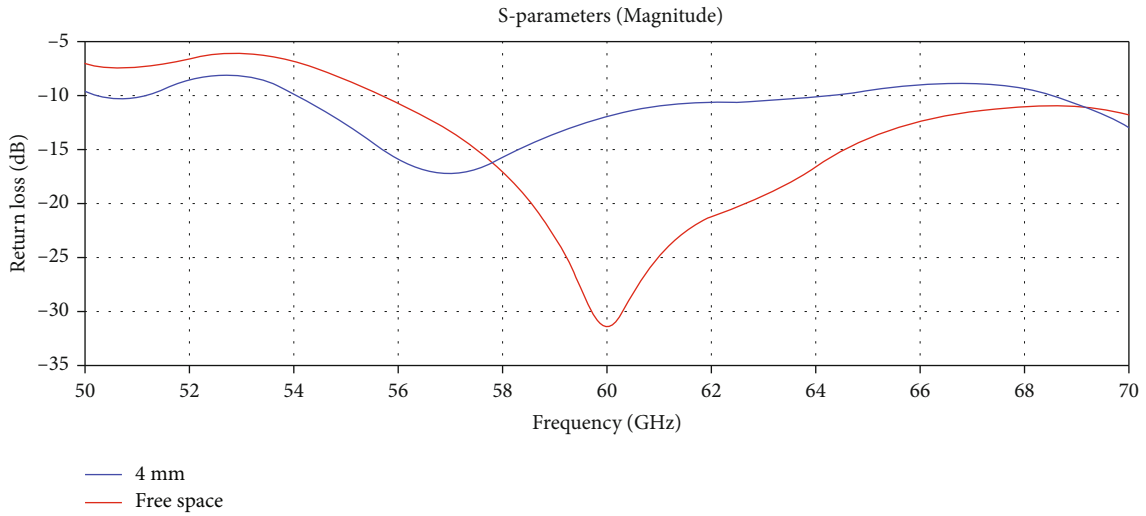

Figure 14: S-parameters comparison between free space and on-body.

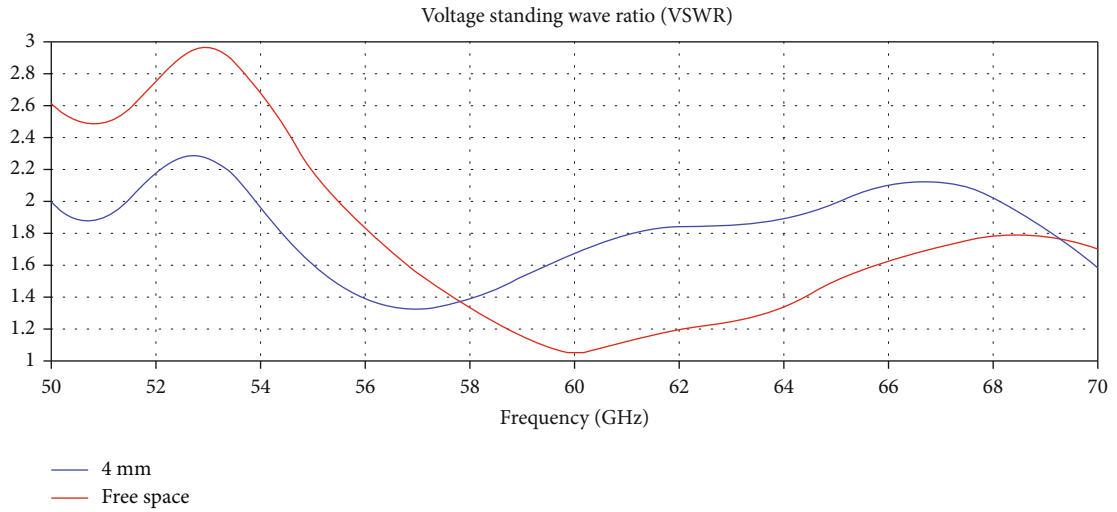

Figure 15: Free-space and on-body VSWR comparison.

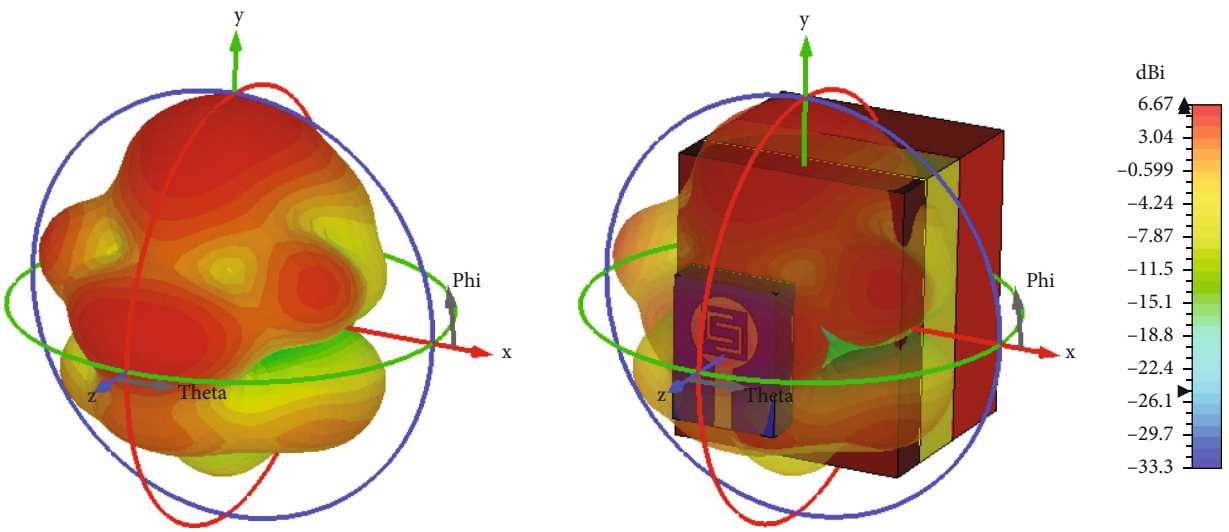

Figure 16: Far-field 3D view on-body 4 mm far without and with structure at 60 GHz.

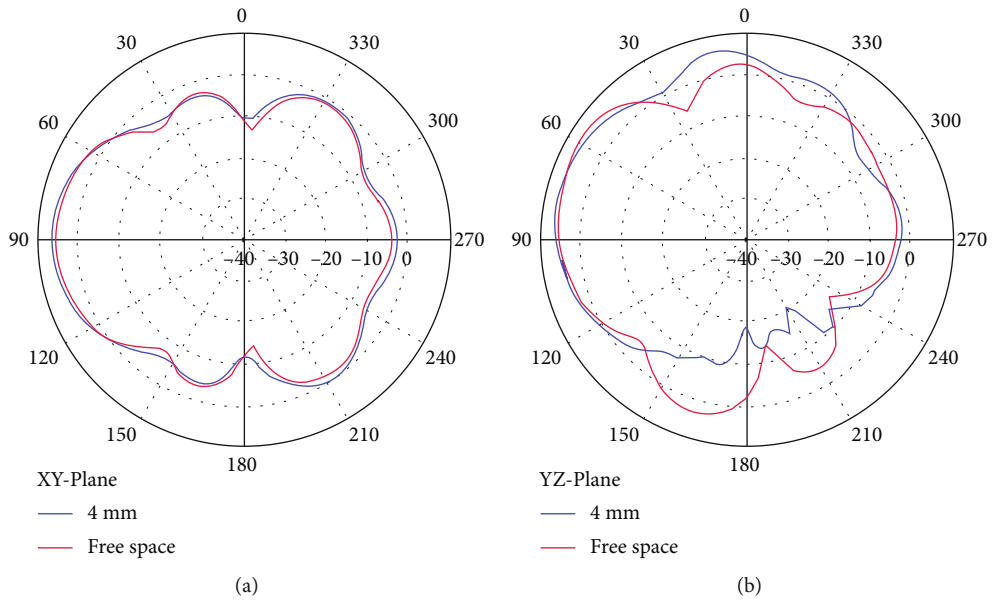

Figure 17: Comparison of the free-space and on-body 2D radiation patterns at 4 mm (a) on the XY plane and (b) on the YZ plane.

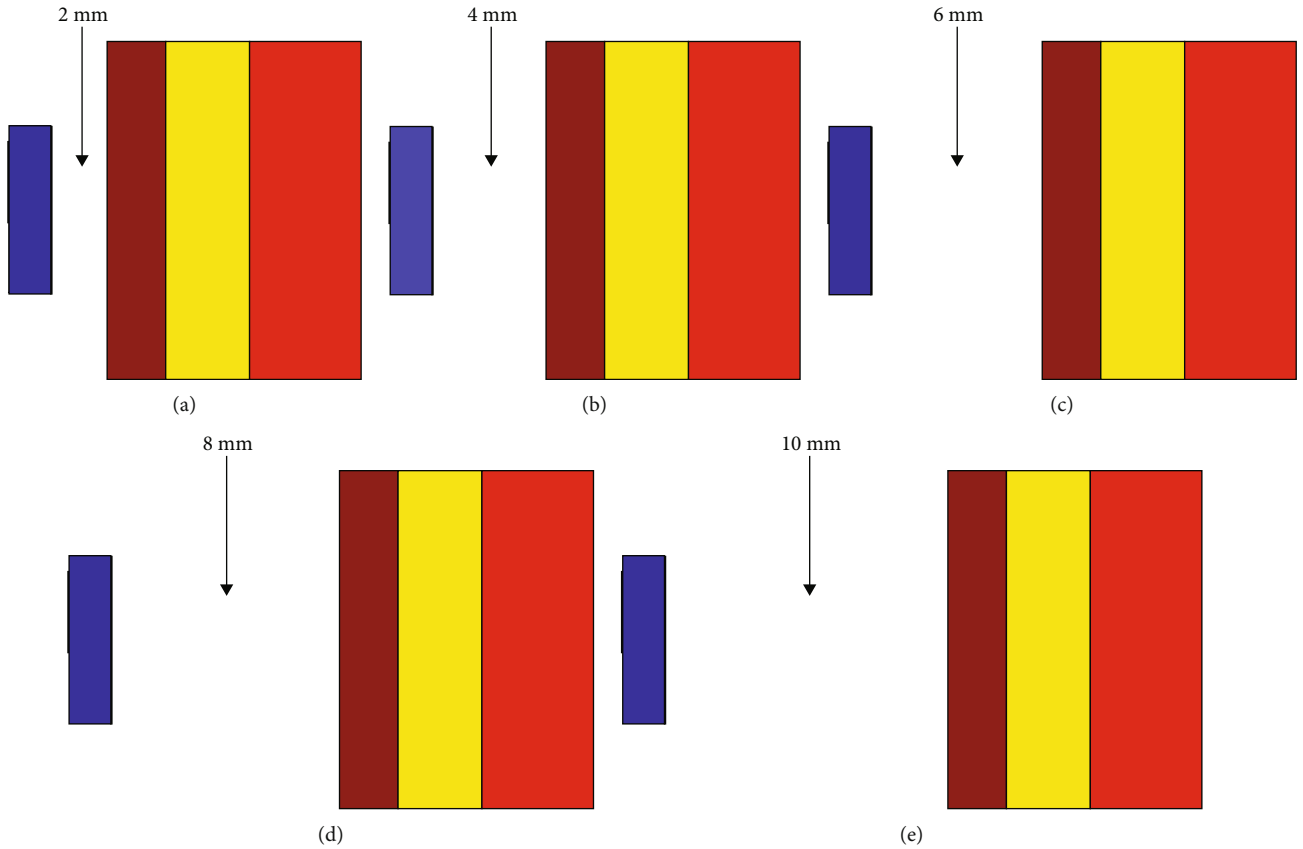

Figure 18: Views looking to the right showing placements of on-body antennas at various distances, including (a) from 2 mm, (b) from 4 mm, (c) from 6 mm, (d) from 8 mm, and (e) from 10 mm.

then compared with one another and the results from the earlier simulations of empty space.

For the return loss results, an antenna kept 8 mm apart from the human body exhibits the lowest return loss, which is slightly below-13 dB. For all the other cases, the return loss value oscillates between -12 dB and -14 dB, which can be seen in the Return Loss comparison plot displayed above (Figure 19). Bandwidths stay almost similar for all the

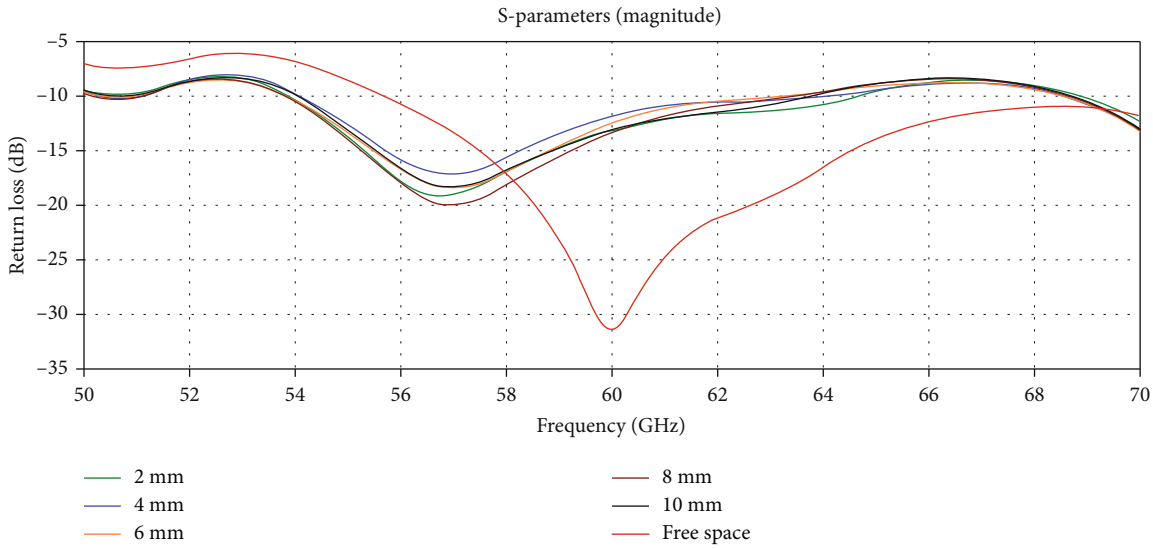

Figure 19: *S*-parameter comparison for varying on-body distances.

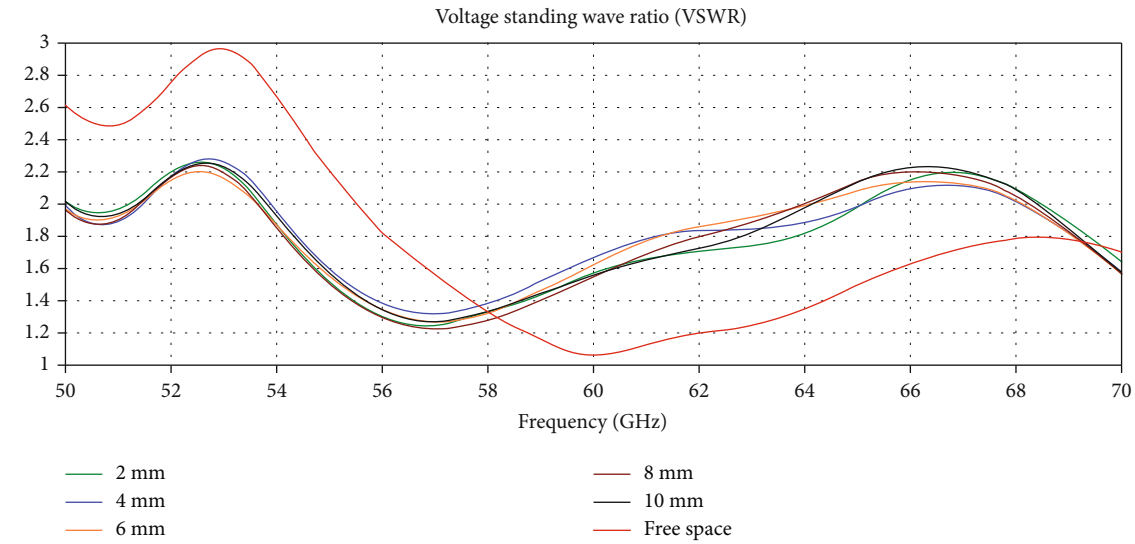

Figure 20: VSWR comparison for various distance on-body.

different on-body simulation scenarios, which vary from 9 GHz to 11 GHz (2 mm). Though the on-body return loss curves show performance differently compared to the free space S11 plot, antenna parameters are still good enough to perform in a body-centric network.

In Figure 20, voltage standing wave ratios were compared for on-body placements of the antenna at different distances. For different distances, on-body VSWR curves show very similar results, but the changes are noticeable when compared to the free-space data. However, for all scenarios, VSWR stayed within 1.5 to 1.7.

Figure 21 depicts how the radiation patterns change as the antenna's distance from the human body increases. In terms of primary lobes, maximum gains, and lobe orientations, it is obvious that the radiation patterns are extremely similar. Figure 19(a) shows the 2D radiation patterns (on the XY plane) of the antenna when it is placed in close proximity to the human torso phantom by varying the distance between them. Patterns are very consistent, even when the on-body distances are varied. Lobe directions remained almost identical while maximum gain values were changed a little bit. Figure 19(b), on the other hand, shows the patterns for YZ planes, which deviate from free space in some specific orientations.

Table 6 contrasts simulations conducted in free-space and on-body. In several on-body simulations, the antenna is positioned at distances of 2 mm, 4 mm, 6 mm, 8 mm, and 10 mm from the torso phantom. Return loss, gain, radiation efficiency, and bandwidth are all taken into account in the comparison. For the return loss comparison, a 2 mm distance from the torso phantom produces a minimum return loss of -44.9 dB. A -32 dB RL was found when the antenna was 6 mm away from the torso, which is the second closest value to the free space simulation. The highest gain was

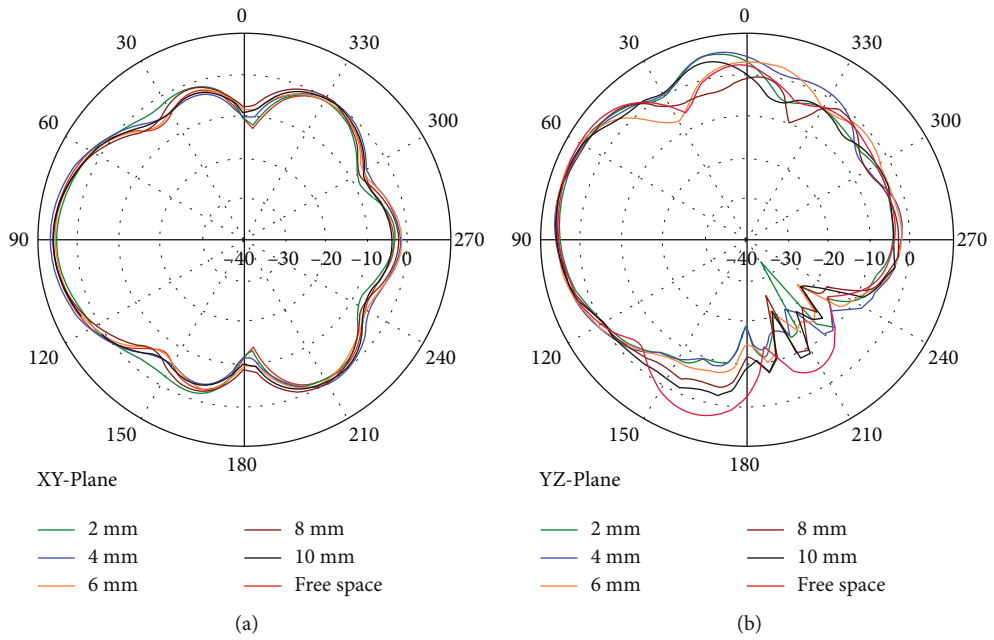

Figure 21: Comparison of the 2D radiation pattern for different on-body distances on the XY plane (a) and the YZ plane (b).

Table 6: Comparison parameters and results.

Parameters	Free-space	On-body 2 mm	On-body 4 mm	On-body 6 mm	On-body 8 mm	On-body 10 m
Return loss(dB)	-31.45	-13.15	-11.99	-12.48	-13.35	-13.17
Bandwidth (GHz)	—	10.77	10.23	9.33	9.54	9.72
Gain (dBi)	6.712	6.293	6.674	6.743	6.400	6.677
Radiation efficiency (%)	84.48	73.78	77.51	76.92	77.41	79.54

Table 7: Comparison with other designs.

	Physical dimension (mm^2)	Return loss (dB)	Gain (dB)	Efficiency	Bandwidth (GHz)	Applied design method	Design complexity
Design 1 [43]	14×12.9	-24	8.66	67.79%	30.068	Slotted patch antenna with partial ground	Q-shaped slot
Design 2 [6]	5.12×8	-32.42	6.071	62.12%	55≤	Multislot Patch antenna	Parasitic element
Design 3 [1]*	3.06×2.28	-13.89	7.13	93%	1.16	Multislot Patch antenna	Multi-dimensional slot
Design 4 [44]	24×17	-14**	4.4	62%	5.8	Substrate-integrated waveguide (SIW) horn antenna	Parallel plate horn
Design 5 (proposed)	6.03×4.5	-12	6.674	77.51%	10.23	Self-complementary patch antenna	Parasitic elements

*Resonant frequency is 60.8 GHz. **Approximate value.

achieved when the antenna was placed at a distance of 6 mm from the body model. Radiation efficiencies increase gradually as the antenna is taken far from the human body. The widest bandwidth was found at a 2 mm distance.

7. Comparison with Other Designs

Here is the comparison table comparing the presented antenna's on-body performance with a few similar antennas designed for BAN/BCN applications operating at 60 GHz. For comparison purposes, a standard 4 mm distance was measured from the human body torso phantom.

In Table 7, the parameters of the proposed antenna for on-body testing were compared with some similar antenna designs. Design 1 presents a partial ground plane and a narrow 'Q'-shaped slot and has a wide bandwidth. Design 2 is a quasiself-complementary antenna with parasitic elements and multiple rectangular slots. For on-body simulations,

both designs used a normal 4 mm spacing from the human body. Design 1 and 2 have used FR4 in their substrates while other designs used RT Duroids (substrate material of design 3 undetermined with a dielectric constant of 2.2). It is clearly visible that the proposed antenna has better radiation efficiency than the other models, except for design3, which has its resonant point slightly above the 60 GHz. However, the presented antenna has a larger bandwidth than designs 3 and 4. Also, from the other parameters, it can be said that the antenna shows better results than average designs.

8. Conclusion

A novel design and study of a self-complimentary miniaturized millimeter wave antenna for wearable applications has been presented. While the proposed antenna design performed significantly well in free-space simulations, the on-body performance of the antenna was good, too. The notable quality of the antenna is that it shows very consistent results for the on-body tests, even though the distances vary, which makes it a potential candidate for the body-centric network (BCN) or wireless body area network (WBAN). Many existing antennas fail to sustain better radiation efficiency while in the near field of a human body, whereas this proposed antenna's recorded minimum on-body efficiency was around 74% for the closest distance. In addition to this, the on-body gain of the antenna shows much wider bandwidths, which is greater than 10 GHz with a gain of -6.674 dB. Aside from that, the antenna performed well in free space simulations, with a gain of more than 6.7 dB and an efficiency of more than 84 percent. All the simulations indicate excellent performance of the antenna throughout the simulation.

This research work is actually based on simulations done in virtual environments due to a lack of opportunities. Simulations done in the CST studio suite have a good reputation in terms of accuracy, which was proven by the countless research done worldwide. Though the antenna was, further parametric improvements could be made in the future by making smaller order arrays with this design.

Data Availability

The data used to support the findings of this study are freely available at http://niremf.ifac.cnr.it/tissprop/

Conflicts of Interest

The authors declare that they have no conflicts of interest to report regarding the present study.

Acknowledgments

This work was funded by the Deanship of Scientific Research at Jouf University under grant No (DSR-2021-02-0390)

References

[1] U. Farooq and G. M. Rather, "A miniaturised Ka/V dual band millimeter wave antenna for 5G body centric network applications," *Alexandria Engineering Journal*, vol. 61, pp. 8089–8096, 2022.

[2] M. Alibakhshikenari, E. M. Ali, M. Soruri et al., "A comprehensive survey on antennas on-chip based on metamaterial, metasurface, and substrate integrated waveguide principles for millimeter-waves and terahertz integrated circuits and systems," *IEEE Access*, vol. 10, pp. 3668–3692, 2022.

[3] K. Neophytou, M. Steeg, A. Stöhr, and M. A. Antoniades, "Compact fixed-beam leaky-wave antenna for 5G millimeter-wave applications," in *2019 13th European Conference on Antennas and Propagation (EuCAP)*, pp. 1–4, Krakow, Poland, 2019.

[4] A. Sebak, "High gain millimeter wave antennas for 5G wireless and security imaging systems," in *2016 33rd National Radio Science Conference (NRSC)*, pp. 2–2, Aswan, Egypt, 2016.

[5] G. Chittimoju and U. Devi, "A comprehensive review on millimeter waves applications and antennas," *Journal of Physics: Conference Series*, vol. 1804, no. 1, article 012205, 2021.

[6] H. M. A. Rahman, M. M. Khan, M. Baz, M. Masud, and M. A. AlZain, "Novel compact design and investigation of a super wideband millimeter wave antenna for body-centric communications," *International Journal of Antennas and Propagation*, vol. 2021, Article ID 8725263, 15 pages, 2021.

[7] A. Ahmed, H. M. Arifur Rahman, and M. M. Khan, "Design and analysis of a compact wideband V-band and W-band antenna for healthcare applications," in *2022 IEEE 12th Annual Computing and Communication Workshop and Conference (CCWC)*, pp. 1043–1048, Las Vegas, NV, USA, 2022.

[8] A. Stohr, C. C. Renaud, D. Rogers et al., "Millimeter-wave photonic components for broadband wireless systems," *IEEE Transactions on Microwave Theory and Techniques*, vol. 58, no. 11, pp. 3071–3082, 2010.

[9] P. Kumar, "Antennas and arrays for 60 GHz high data rate wireless applications," *International Journal on Communications Antenna and Propagation (IRECAP)*, vol. 9, no. 4, pp. 255–262, 2019.

[10] B. Bosco, R. Emrick, S. Franson, J. Holmes, and S. Rockwell, "Emerging commercial applications using the 60 GHz unlicensed band: opportunities and challenges," in *2006 IEEE Annual Wireless and Microwave Technology Conference*, pp. 1–4, Clearwater Beach, FL, USA, 2006.

[11] N. Guo, R. C. Qiu, S. S. Mo, and K. Takahashi, "60-GHz millimeter-wave radio: principle, technology, and new results," *EURASIP Journal on Wireless Communications and Networking*, vol. 2007, no. 1, Article ID 068253, 2006.

[12] B. Yang, Z. Yu, Y. Dong, J. Zhou, and W. Hong, "Compact tapered slot antenna array for 5G millimeter-wave massive MIMO systems," *IEEE Transactions on Antennas and Propagation*, vol. 65, no. 12, pp. 6721–6727, 2017.

[13] B. Kibret, A. K. Teshome, and D. T. H. Lai, "Human body as antenna and its effect on human body communications," *Progress In Electromagnetics Research*, vol. 148, pp. 193–207, 2014.

[14] S. Chowdhury and K. Ali, "Effects of human body on antenna performance: a quantitative study," in *2016 19th International Conference on Computer and Information Technology (ICCIT)*, pp. 108–112, Dhaka, Bangladesh, 2016.

[15] Y. Hao, "Antennas and propagation for body centric wireless communications," in *2011 IEEE International Conference on Microwave Technology & Computational Electromagnetics*, p. 3, Beijing, China, 2011.

[16] K. Fujii, K. Ito, and S. Tajima, "A study on the receiving signal level in relation with the location of electrodes for wearable devices using human body as a transmission channel," in *IEEE Antennas and Propagation Society International Symposium. Digest. Held in conjunction with: USNC/CNC/URSI North American Radio Sci. Meeting (Cat. No.03CH37450)*, Columbus, OH, USA, 2003.

[17] T. G. Zimmerman, "Personal area networks: near-field intrabody communication," *IBM Systems Journal*, vol. 35, no. 3.4, pp. 609–617, 1996.

[18] T. G. Zimmerman, J. R. Smith, J. A. Paradiso, D. Allport, and N. Gershenfeld, "Applying electric field sensing to human-computer interfaces," in *Proceedings of the SIGCHI conference on Human factors in computing systems - CHI '95*, pp. 280–287, Denver, Colorado, USA, May 1995.

[19] W. Wu, Y.-B. Li, R.-Y. Wu, C.-B. Shi, and T.-J. Cui, "Band-notched UWB antenna with switchable and tunable performance," *International Journal of Antennas and Propagation*, vol. 2016, Article ID 9612987, 6 pages, 2016.

[20] H. Rahman and M. Khan, "Design and analysis of a compact band notch UWB antenna for body area network," *Journal of Electromagnetic Analysis and Applications*, vol. 10, no. 9, pp. 157–169, 2018.

[21] V. Kumar and B. Gupta, "Design aspects of body-worn UWB antenna for body-centric communication: a review," *Wireless Personal Communications.*, vol. 97, no. 4, pp. 5865–5895, 2017.

[22] T. Kumpuniemi, M. Hamalainen, K. Y. Yazdandoost, and J. Iinatti, "CATEGORIZED UWB on-body radio channel modeling for WBANS," *Progress In Electromagnetics Research B*, vol. 67, pp. 1–16, 2016.

[23] E. Miralles, C. Andreu, M. Cabedo-Fabrés, M. Ferrando-Bataller, and J. F. Monserrat, "UWB on-body slotted patch antennas for in-body communications," in *2017 11th European Conference on Antennas and Propagation (EUCAP)*, pp. 167–171, Paris, France, 2017.

[24] A. Alomainy, A. Sani, A. Rahman, J. G. Santas, and Y. Hao, "Transient characteristics of wearable antennas and radio propagation channels for ultrawideband body-centric wireless communications," *IEEE Transactions on Antennas and Propagation*, vol. 57, no. 4, pp. 875–884, 2009.

[25] M. Ur-Rehman, N. A. Malik, X. Yang, Q. H. Abbasi, Z. Zhang, and N. Zhao, "A low profile antenna for millimeter-wave body-centric applications," *IEEE Transactions on Antennas and Propagation*, vol. 65, no. 12, pp. 6329–6337, 2017.

[26] N. Chahat, M. Zhadobov, and R. Sauleau, "Antennas for body centric wireless communications at millimeter wave frequencies," in *Progress in Compact Antennas*, IntechOpen, London, UK, 2014.

[27] J. Puskely, M. Pokorny, J. Lacik, and Z. Raida, "Wearable disc-like antenna for body-centric communications at 61 GHz," *IEEE Antennas and Wireless Propagation Letters*, vol. 14, pp. 1490–1493, 2015.

[28] V. S. Ubale and O. S. Lamba, "Flexible wearable antennas for body area network," *International Journal of Engineering Science*, vol. 8, no. 5, pp. 1561–1565, 2020.

[29] Z. H. Jiang, Z. Cui, T. Yue, Y. Zhu, and D. H. Werner, "Compact, highly efficient, and fully flexible circularly polarized antenna enabled by silver nanowires for wireless body-area networks," *IEEE Transactions on Biomedical Circuits and Systems*, vol. 11, no. 4, pp. 920–932, 2017.

[30] A. Brizzi, A. Pellegrini, L. Zhang, and Y. Hao, "Woodpile EBG-based antennas for body area networks at 60GHz," in *2012 4th International High Speed Intelligent Communication Forum*, pp. 1–4, Nanjing, China, 2012.

[31] M. Alibakhshikenari, B. S. Virdee, S. Salekzamankhani et al., "High-isolation antenna array using SIW and realized with a graphene layer for sub-terahertz wireless applications," *Scientific Reports*, vol. 11, no. 1, article 10218, 2021.

[32] M. Alibakhshikenari, B. S. Virdee, A. A. Althuwayb et al., "Study on on-chip antenna design based on metamaterial-inspired and substrate-integrated waveguide properties for millimetre-wave and THz integrated-circuit applications," *J Infrared MilliTerahz Waves*, vol. 42, no. 1, pp. 17–28, 2021.

[33] M. Alibakhshikenari, B. S. Virdee, C. H. See, R. A. Abd-Alhameed, F. Falcone, and E. Limiti, "High-isolation leaky-wave array antenna based on CRLH-metamaterial implemented on SIW with ±30o frequency beam-scanning capability at millimetre-waves," *Electronics*, vol. 8, no. 6, p. 642, 2019.

[34] M. Alibakhshikenari, B. S. Virdee, C. H. See, R. A. Abd-Alhameed, F. Falcone, and E. Limiti, "Super-wide impedance bandwidth planar antenna for microwave and millimeter-wave applications," *Sensors (Basel).*, vol. 19, no. 10, p. 2306, 2019, Published 2019 May 19.

[35] M. Alibakhshikenari, B. S. Virdee, C. See et al., "Beam-scanning leaky-wave antenna based on CRLH-metamaterial for millimetre- wave applications," *IET Microwaves, Antennas & Propagation*, vol. 13, no. 8, pp. 1129–1133, 2019.

[36] M. Alibakhshikenari, B. S. Virdee, L. Azpilicueta et al., "A comprehensive survey of "metamaterial transmission-line based antennas: design, challenges, and applications"," *IEEE Access*, vol. 8, pp. 144778–144808, 2020.

[37] M. Ur-Rehman, M. Adekanye, and H. T. Chattha, "Tri-band millimetre-wave antenna for body-centric networks," *Nano Communication Networks*, vol. 18, pp. 72–81, 2018.

[38] H. Shawkey and D. Elsheakh, "Multiband dual-meander line antenna for body-centric networks' biomedical applications by using UMC 180 nm," *Electronics*, vol. 9, no. 9, p. 1350, 2020.

[39] X. Y. Wu, Y. Nechayev, and P. S. Hall, "Antenna design and channel measurements for on-body communications at 60 GHz," in *2011 XXXth URSI General Assembly and Scientific Symposium*, pp. 1–4, Istanbul, Turkey, 2011.

[40] T. Ramachandran, M. R. I. Faruque, and M. T. Islam, "A dual-band polarization-independent left-handed symmetrical metamaterial for communication system application," *Journal of Materials Research and Technology*, vol. 15, pp. 731–744, 2021.

[41] P. Kumar, T. Ali, and A. Sharma, "Flexible substrate based printed wearable antennas for wireless body area networks medical applications (review)," *Radioelectron.Commun.Syst.*, vol. 64, no. 7, pp. 337–350, 2021.

[42] S. G. Kirtania, A. W. Elger, M. R. Hasan et al., "Flexible antennas: a review," *Micromachines*, vol. 11, no. 9, p. 847, 2020.

[43] M. M. Khan, K. Islam, M. N. A. Shovon, M. Baz, and M. Masud, "Design of a novel 60 GHz millimeter wave Q-slot antenna for body-centric communications," *International Journal of Antennas and Propagation*, vol. 2021, Article ID 9795959, 12 pages, 2021.

[44] S. Razafimahatratra, J. Sarrazin, A. Benlarbi-Delai et al., "On-body propagation characterization with an H-plane substrate integrated waveguide (SIW) horn antenna at 60 GHz," in *2015 European Microwave Conference (EuMC)*, pp. 211–214, Paris, France, 2015.